Modeling and Simulation of 3D Surface Finish of Grinding

AMM Sharif Ullah, Jun'ichi Tamaki and Akihiro Kubo

Kitami Institute of Technology, 165 Koen-cho, Kitami, Hokkaido 090-8507, Japan

{ullah,tamaju,kuboak}@mail.kitami-it.ac.jp

Keywords: Grinding, 3D Surface Finish, Stochastic Process, Digital Machining.

Abstract. This paper describes a method for modeling and simulation of 3D surface finish for precision grinding from the perspective of digital machining. The idea is to produce an active working model so that it becomes useful for both man and machine during reuse of machining resources. 3D surface finish consists of three stochastic features called trend, irregularity, and burst. Mathematical procedure is developed to model and simulate these features independently. A simulation tool is developed to implement the method. The simulation result is compared with real 3D surface finish showing the effectiveness of the method.

Introduction

Nowadays, a concept called *digital machining* has become an important issue for the machining community. The challenge is to integrate human and machining resources using computer networking. Various works has been done in this area. Few of them are described below in brief. Matsuda et al. [z] proposed a digital machining information system based on STEP (ISO10303) and ISO14649 for supporting real-virtual machining operations. This system requires integration of machine tool, cutting tool, workpiece, machining process, and fixture models in a systematic manner. The details of machine tool model are shown in [z]. Bui and Vorburger [z] developed a Web-based surface metrology algorithm testing system, which can be accessed through http://syseng.nist.gov/VSC/jsp. Using this system one can upload his/her surface finish data using a prescribed file-format and get the values of surface texture parameters in accordance with ASME B46.1 (ISO42287, ISO4288, and ISO5436-2). This way one can confirm whether or not the system he/she uses for surface metrology is a reliable one. Butala and Sluga [z] developed a networking concept for effective sharing of manufacturing knowledge among stakeholders (SMEs, Machine tool makers, cutting tool makers, etc.) using Internet. The main building block of such a network is called autonomous work system. An autonomous work system carries the functionalities and competencies to perform a manufacturing operation. It also acts as an autonomous information system supporting autonomous decision-making and cooperation in the network. To implement this networking concept it is however important to deal with the data of machining operations that includes tooling information, cutting condition information, workpiece information and so on [z]. National Institute of Advanced Industrial Science and Technology in Japan developed a digital machining system that can be accessed through http://www.monozukuri.org/db-dmrc/. This provides basic and advanced operational information of various machining processes (turning, milling ,drilling, grinding, polishing, coating, leaser cutting, etc.) to help human users.

Despite the aforementioned progresses in digital machining, more research is needed. The rationale is explained, as follows.

The main body of machining knowledge comes from the machining experiments done by independent investigators. If such experimental results are not made both human and machine readable from the very beginning, then it would be difficult to make such technical resources useful for human and machine while reusing through computerized network or through any other means. In this respect, intelligent systems are needed to create reliable models of important results like 3D surface finish, cutting force, tool wear, etc. The models can be integrated with a digital machining library (e.g., http://www.monozukuri.org/db-dmrc/) within the framework of collaborative working environment empowered by ambient intelligence [z]. From such a library these models can be downloaded for human use (research community, industry), for human and machine use (process planning, condition monitoring), or even for machine use (automation, autonomous robots). This aspect is illustrated in Fig. 1.

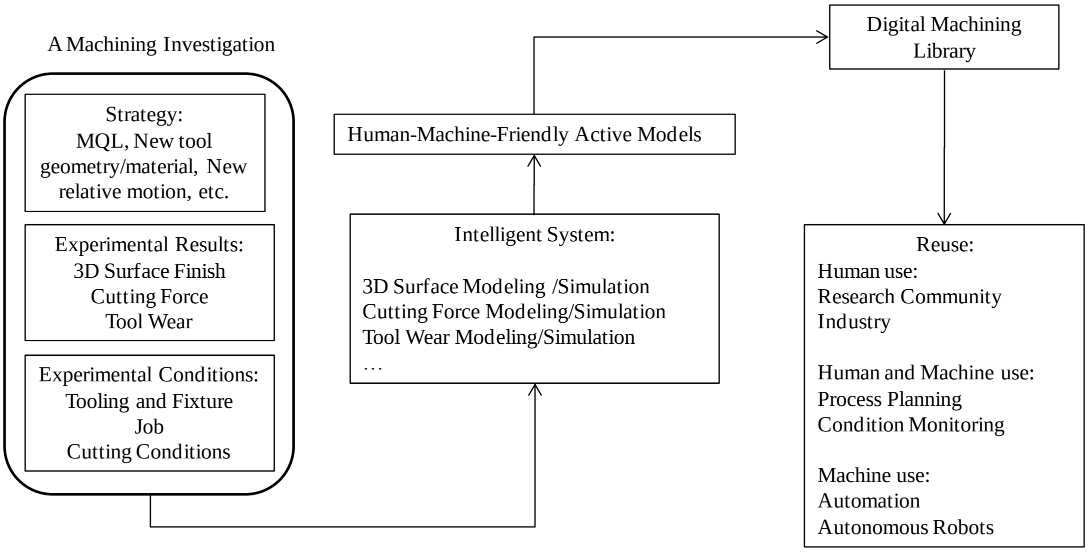

Fig. 1 Link between machining investigation and reuse of machining resource.

However, 3D surface finish is one of the important results of a grinding operation. An investigator uses a set of feasible cutting conditions under a specific cutting strategy and identifies a way to produce a desirable surface finish. The results of such investigations can be used later for process planning, condition monitoring, sharing information with peers in the field, and helping industry to develop commercial systems, and so on. This means that the results of 3D surface will be reused by humans and machines. As a result, a model is needed that makes the results of 3D surface finish equally comprehensible for human users and machines. From this perspective, this study describes a method for modeling 3D surface finish of a grinding operation. The remainder of this paper is organized as follows: Section 2 defines the concepts that is used to process 3D surface finish data. Section 3 describes typical features of a 3D surface data. Section 4 describes a stochastic model of 3D surface and discusses the results, which is followed by the conclusion of this study.

Preliminaries

Consider that there is *sequence of points*: $u(1),\ldots,u(i),\ldots,u(n)$ so that $((u(i)\in\Re, \forall i=1,\ldots,n)$. The *time series* plot consists of plotting the points $(1,u(1)),\ldots,(i,u(i)),\ldots,(n,u(n))$. The first order *return map* consists of plotting the points $(u(1),u(2)),\ldots,(u(i),u(i+1)),\ldots,(u(n-1),u(n))$. Consider that there is a sequence of intervals $A_0,A_0+1\times\Delta,\ldots,A_0+j\times\Delta,\ldots,A_0+m\times\Delta$, wherein $A_0=min(u(i)-\varepsilon_0$ and $A_0+m\times\Delta=max(u(i)+\varepsilon_1$. The *probability curve* denoted by Pr(A) represents the probability of points of a return map being in the square-box of size A, where $A= A_0+j\times\Delta$ $(\forall j=1,2,\ldots,m)$. Figure 2 shows these three plots (*time series*, *return map*, and *probability curve*) for a hypothetical case.

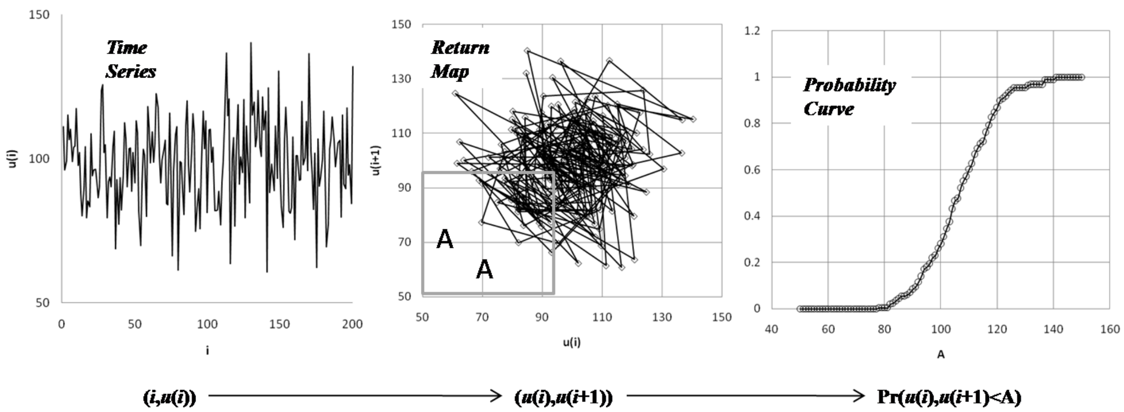

Fig. 2. Different plots for visual inspection.

A sequence of points $v(1),...,v(i),...,v(n)$ is said to an "acceptable working model" of $u(1),...,u(i),...,u(n)$ if the time series plots and return maps look alike and the probability curves are very close to each other as well. For example, consider the case shown in Fig. 3, wherein the time series plots, return maps, and probability curves of $u(1),...,u(i),...,u(n)$ and $v(1),...,v(i),...,v(n)$ are shown in a single graph, respectively. From the visual inspections of these plots it is clear that $v(1),...,v(i),...,v(n)$ is not a good model of $u(1),...,u(i),...,u(n)$.

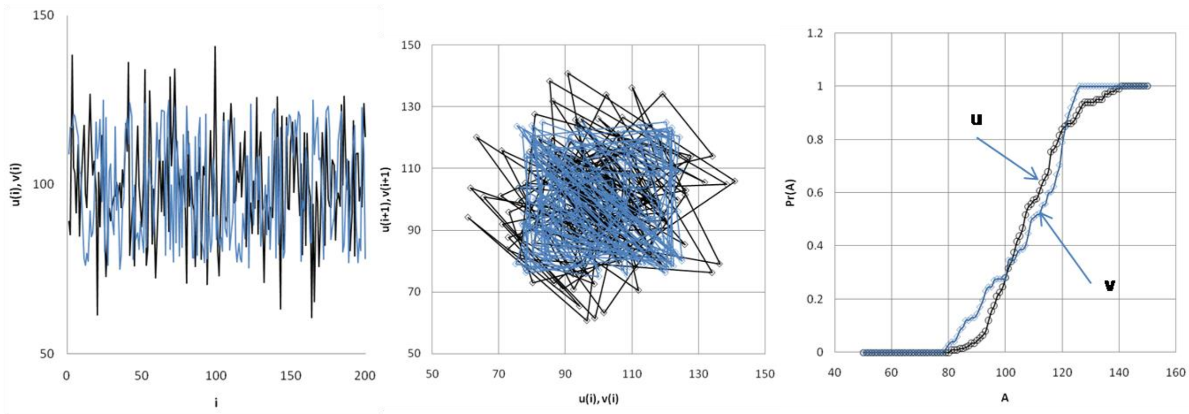

Fig. 3. Modeling effectivenss.

This visual technique is used hereinafter to develop acceptable working models of a given 3D surface. Before explaining the modeling procedure, some of the salient features of 3D surface finish are explained in the following section.

Features of 3D Surface Finish

This section describes some of the salient features of 3D surface finish for the sake of modeling and simulation. Figure 4 shows a typical case of 3D surface finish data acquisition procedure from a grinding investigation.

It is well-know that grinding is a very complex material removal process [z put references Tamaki et al….]. The interaction between a grinding wheel surface and workpiece surface is somewhat impossible to model by purely engineering-science-based approaches. In most cases, various computing paradigms are integrated to model various aspects of grinding process. See [z] for more details on this issue. However, the surface of a grinding wheel is very complex and requires stochastic process to create a realistic model of grinding [z]. When such a wheels interact with a workpiece, a highly nonlinear cutting forces evolves [z]. As a result, the surface finish becomes quite chaotic in nature. Unlike a surface roughness profile, 3D surface finish is supposed to have all topological components like roughness, waviness, trend, and lay. This makes surface roughness modeling techniques [z] somewhat inapplicable for 3D surface finish. Many authors have developed models for 3D surface finish. One of the effective approaches is to use stochastic process like Gaussian process [z]. In the proposed model, a clear procedure is not found which can be used by an ordinary user to comprehend the whole process of modeling and himself/herself involved in the model. Moreover, there is no indication how these models should be incorporated into a collaborative environment of manufacturing or digital machining.

However, an investigator first determines a strategy to apply relative motions between a grinding wheel and workpiece and adjust these motions to get a better surface finish. The surface finish is measured by using non-contact surface metrology instrument (e.g., Mitaka NH-2SP). The instruments are equipped with software packages that help visualize the 3D surface finish for mainly human use (e.g., MitakaMap). Some instruments provides a electronic file wherein the 3D surface data in term of 3D Cartesian coordinate system (*x*,*y*,*z*) are saved for sake of further analysis. The *x*- and *y*-coordinates of the data points are actually an x-y grid as shown in Fig. 4 and *z*-coordinate actually contains valuable information of the surface. This grid and *z*-coordinate can be used to develop models for 3D surface finish.

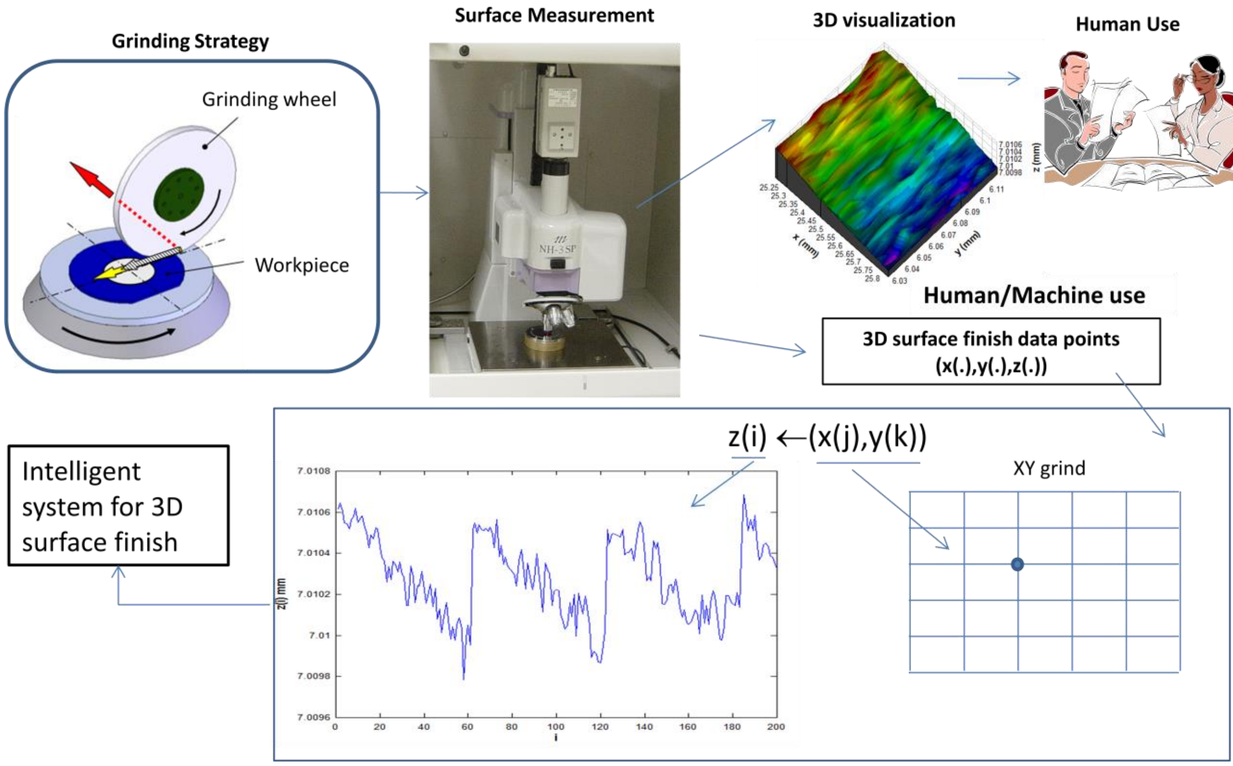

Fig. 4. 3D surface finish data acquisition.

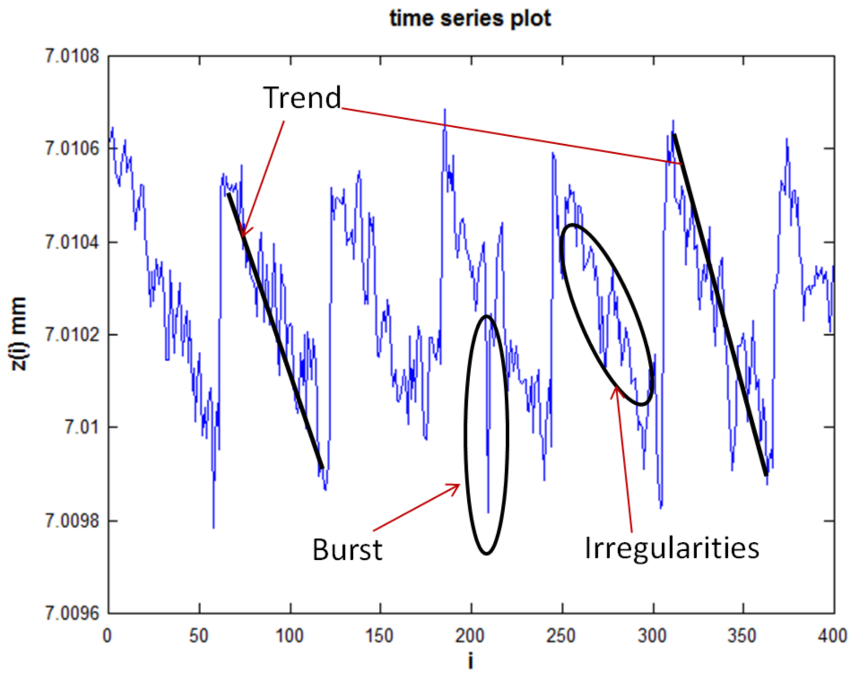

Figure 5. Features of surface finish.

The time series plot of *z*-coordinate provides valuable insights into the features of a surface finish. For example, consider the time series plot of *z*-coordinate shown in Fig. 5. As seen from Fig. 5, in the time series plot a cyclical patter repeats after a definite time span (i.e., after certain count of *i*). In each cycle there are some stochastic features called *trend*, *irregularity*, and *burst*. For this particular case, the trend is a straight-line with a *negative slope* and the slope *slightly changes* from cycle to cycle. This is perhaps a result of an alignment error that persisted during the operation, or is perhaps a result of a linearly varying depth of cut, or is perhaps a result of any other valid reasons. One the other hand, the *irregularly* is rather chaotic in nature. From the eye estimation it seems that a random process has is associated that created the *irregularity*. Sometimes, a significantly large but localized irregularity appears. This forms a *burst*. As such, a *burst* occurs rarely at a selective position of a cycle.

From the above explanation is it clear that a set of mathematical procedures is needed to model *trend*, *irregularity*, and *burst* independently. The results of such independent mathematical procedures can be integrated to model the *z*-coordinate. This can be further integrated with an *x-y* grid to produce the 3D model of a given surface finish. The next section shows the details of the aforementioned modeling technique.

Modeling

To model a straight-line *trend* the following mathematical setting can be used.

$$\begin{aligned}
&\textit{define}: \\
&x(1)=x_s \leftarrow N(\mu_s,\sigma_s) \quad x(n)=x_f \leftarrow N(\mu_f,\sigma_f) \\
&\textit{for} \quad i=2\ldots n \quad \textit{do} \quad x(i)=x(i-1)+\frac{x_s-x_f}{n-1}
\end{aligned} \tag{1}$$

According to (1), two values of x (x_s and x_f) are created using Gaussian processes $N(\mu_s,\sigma_s)$ and $N(\mu_f,\sigma_f)$ for a given span i=1, and i=n. From these points, the slope of the trend and the coordiante of the points on the trend-line (i,$x(i)$) are cacluated recurrsively. This procedure is applied to model the trend of the time series plot shown in Fig. 5. This results is shown in Fig. 6.

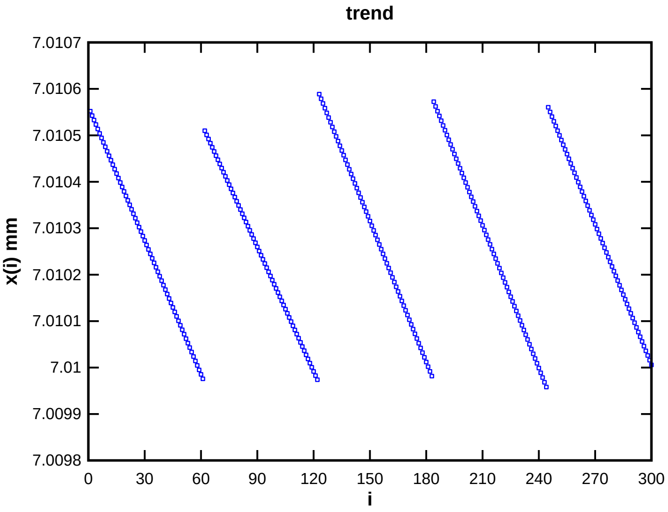

Figure 6. Modeling straight-line *trend*.

As seen from Fig. 6, the slope of the trend slightly varies from cycle to cycle, which is desirable for this particular case.

To model the *irregularity* the following mathematical setting can be used.

$$
\begin{aligned}
&\textit{define}:\\
&a=[a_L,a_H]\quad b=[b_L,b_H]\quad A=[A_L,A_H]\quad B=[B_L,B_H]\\
&\textit{for}\quad i=1\ldots n\\
&\textit{do}\quad y(i)=a\sin\left(\frac{2\pi}{A}i\right)\pm b\cos\left(\frac{2\pi}{B}i\right)
\end{aligned}
\qquad (2)
$$

According to (2), $y(i)$ varies irregularly as the amplitude and period of the periodic functions are varied randomly. Figure 7 shows an instance of $y(i)$, where ± is determined at random, A is varied radomly between the integers in the range [10,20], B is kept 20, and a and b are varied randomly between [0.00001,0.00012] and [0.00001,0.0001], respectivly.

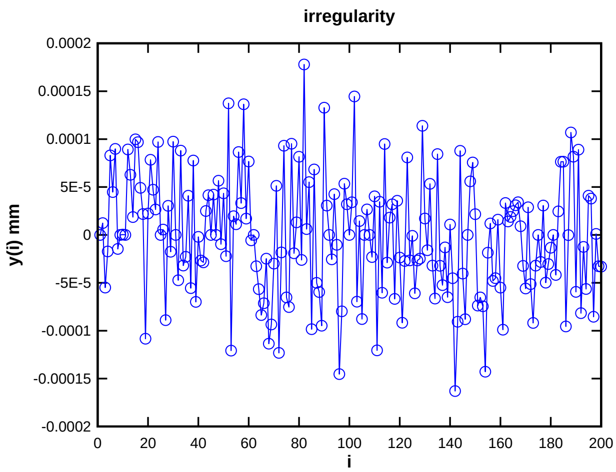

Fig. 7. Modeling *irregularity*.

To model the *burst*, the following mathematical setting can be used.

$$\begin{array}{l} \textit{define}: \\ P_B \leftarrow [n_1, n_2], L_B \leftarrow [0,1], M_B \leftarrow [x_L, x_H] \\ \textit{for} \quad i = 1 \ldots n \\ \textit{do} \quad x'(i) = M_B \quad \textit{if}\,(i = P_B) \wedge (r_i < L_B) \\ \textit{otherwise} \quad \textit{do} \quad x'(i) = x(i) \end{array} \tag{3}$$

According to (3), to produce a *burst* it is important to assign three variables called position of the burst (P_B) (an integer), likelihood of burst (L_B), and magnitute of burst (M_B). When a randomly generated value (r_i) remains less than L_B and the index i is equal to P_B then $x(i)$ changes to M_B. Otherwise, $x(i)$ remains the same. Note that the formulation in (3) associates burst with trend as defined in (1). This can be associated with irregulaty defined in (2), instead. Since these features are modeled independenly, the results remains the same. However, Fig. 8 shows an typical simualtion result when P_B=[35,40], M_B=[7.00975,7.01], and L_B=0.3.

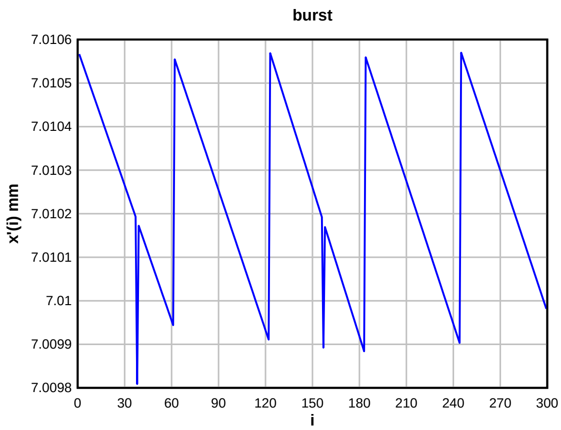

Fig. 8. Modeling burst.

To model *z*-coordinate of 3D surface finish, the following formulation can be used.

$$z(i) = x'(i) + y(i) \tag{4}$$

Figure 9 shows an instance of simulated $z(i)$ in accordance with (4). As expected, the time series plot shown in Fig. 9 has localized *burst*, stochastic *irregularity*, and straight-line *trend*.

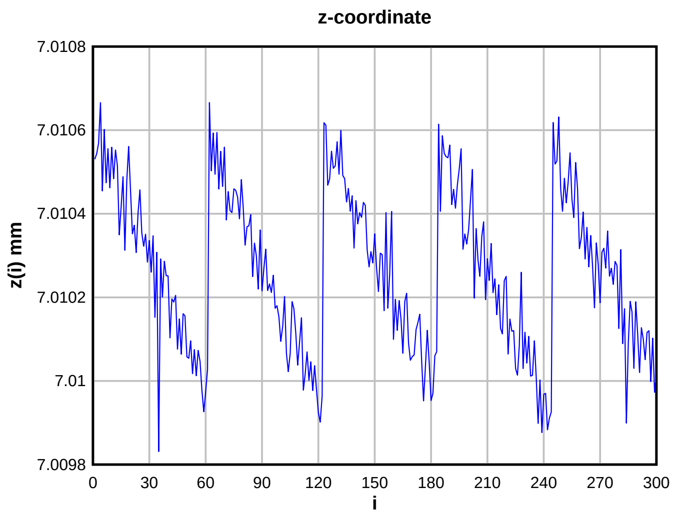

Fig. 9. Modeling *z*-coordinate.

Results and Discussion

A simulation tool has been developed to implement the modeling technique described in the previous section. Figure 10 shows the snapshot of the user interface of the simulation tool. As seen from Fig. 10, the user can fix the values of the parameters defined in (1)-(3). Using the user-defined values of the parameters, the tool simulates ten cycles of *z*-coordinate independently and displays the simulated and real *z*-coordinates in term of time series, return map, and probability curve. Using the visual inspection, a user can adjust the values of parameters and finally identify an active working model for z-coordinates.

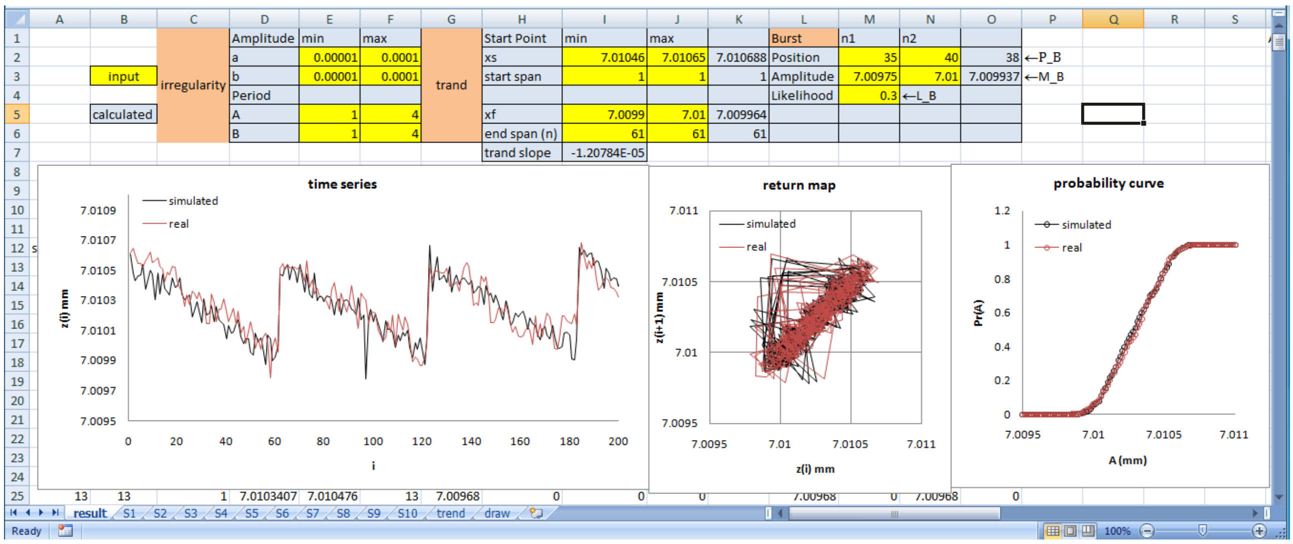

Fig. 10. Simulation tool.

It is useful to adjust the parameters of the trend first. Afterward the parameters of the irregularity can be adjusted followed by the adjustment of the burst. The parameter settings shown in Fig. 10 provide a close correlation between real and simulated *z*-coordinates, as can be verified from the plots shown in Fig. 11. The time series plot of the simulated *z*-coordinate exhibits a burst not in the same location as it is found in the real signal (see the time series plot in Fig. 11). The irregularity sometimes resembles and sometimes not, as seen from the time series in Fig. 11. The trend also shows similar resemblance. The return map of the simulated *z*-coordinate shown in Fig. 11 is very similar to that of the real one. This is also true for the probability curves shown in Fig. 11.

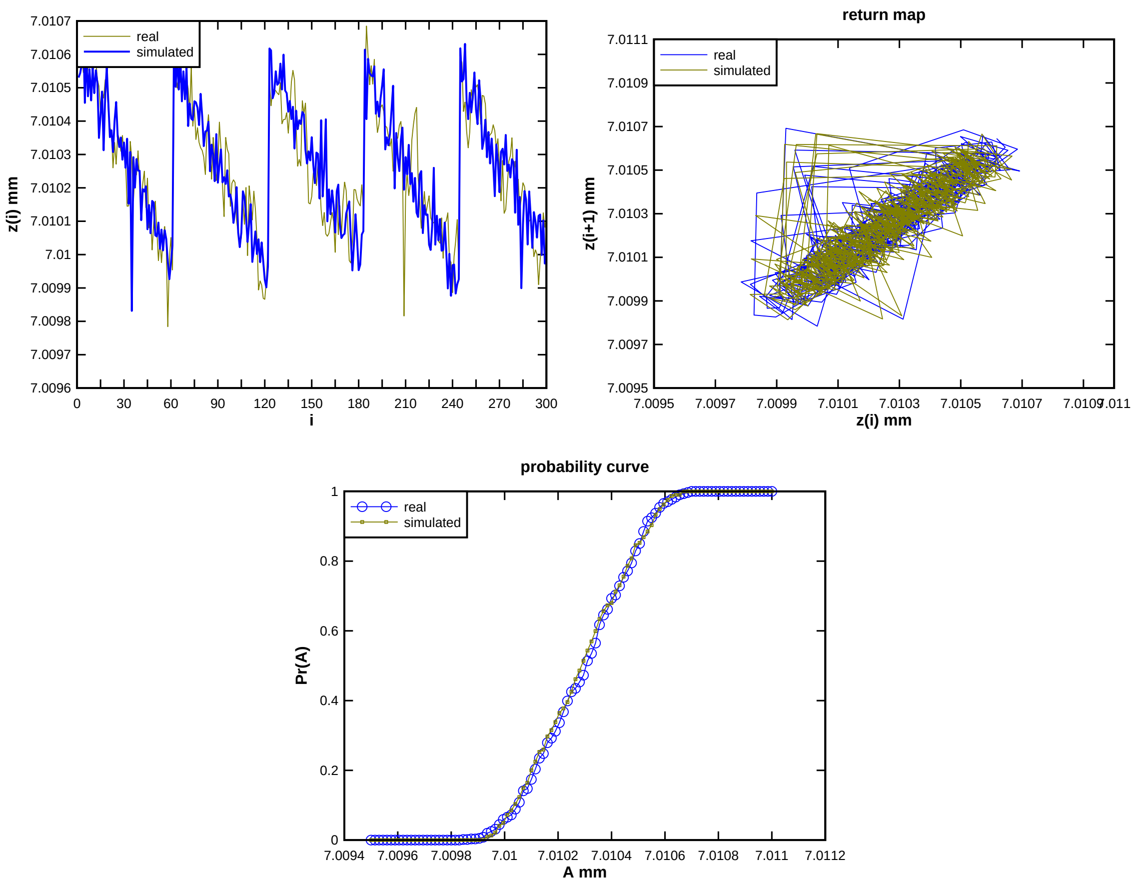

Fig. 11. Correlation between real and simulated *z*-coordinates.

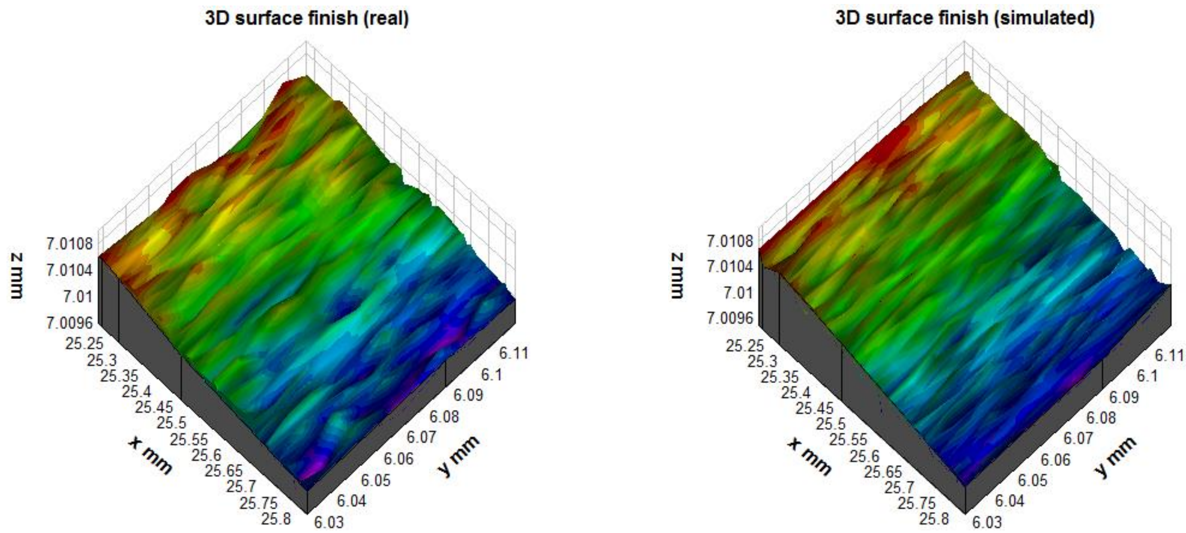

Fig. 12. 3D plots of real and simulated surface finish.

When the 3D plots of real and simulated surfaces are compared, as it is shown in Fig. 12, it is found the simulated surface is remarkably similar to the real surface. However, peaks and valleys in the real surface are wider than that of simulated surface. This means slight modification in the model of irregularity is needed. One of the ways might to introduce an interpolation procedure to create more points between $y(i)$ and $y(i+1)$ as defined in (2) and use the modified set of points to create irregularity for z-coordinate. This issue remains open for further research, however.

Reference

T. Matsuda, F. Tanaka, M. Onosato and H. Date. Development of a Digital Machining Information Model to Support a Real-Virtual Machining System, *Journal of Advanced Mechanical Design, Systems, and Manufacturing*, Vol. 2(4) (2008), p.597-608.

S. H. Bui and T. V. Vorburger, Surface metrology algorithm testing system, *Precision Engineering*, Vol. 31(3) (2007), p. 218-225.

P. Butala and A. Sluga, Autonomous Work Systems in Manufacturing Networks, *CIRP Annals-Manufacturing Technology*, Vol.55(1) (2006), p.521-524.

Z. Judez, A. Sluga, P. Butala, J. Kopac and J. Peklenik, Toward a Web-Based Machinability Data Service, *Proceedings of the 6th CIRP Conference in Intelligent Computation in Manufacturing Engineering*, 23-25 July, 2008, Naples, Italy, p. 141-146.

K. Shiyouzi (Ed.). *Ultra-Precision Machining and Non-Spherical Surface Machining*, NTS Corporation, Tokyo, 2004. (In Japanese).

M. Higuchi, A. Yano, N. Yamamoto, T. Yamaguchi, E. Eookai, N. Matsumori, and I. Yoshizawa, Development of Design Technology of Porous Superfinishing Stone Using Fractal Geometry (1st Report): Construction of Characteristic Equations Required for Design, *Journal of the Japan Society of Precision Engineering*, Vol.65(6), 1999, 857-861. (In Japanese).

M. Higuchi, T. Tomiyama, N. Matsumori and H. Ogura, Geometric Modeling of Vitrified Superabrasive Stone Surface, *Transaction of the Japan Society of Mechanical Engineers*, Series C, Vol.73(732), 2007, 207-212. (In Japanese).

T. Yamaguchi, M. Higuchi, S. Shimada, N. Matsumori, I. Yoshizawa and H. Ogura, Fractal modeling method for 3D structure of vitrified-bonded wheel, Precision Engineering, Vol.31(1), 2007, 40-46.

E. Brinksmeier, J.C. Aurich, E. Govekar, C. Heinzel, H.-W. Hoffmeister, F. Klocke, J. Peters, R. Rentsch, D.J. Stephenson, E. Uhlmann, K. Weinert and M. Wittmann, Advances in Modeling and Simulation of Grinding Processes, *CIRP Annals - Manufacturing Technology*, Vol.55(2), 2006, p. 667-696.

D. Biermann and T. Mohn, A Geometric-Kinematical Approach for the Simulation of Complex Grinding Process, *Proceedings of the 6th CIRP International Conference on Intelligent Computation in Manufacturing Engineering*, 23-25 July, 2008, Naples, Italy, p.401-405.

A.M.M.S. Ullah and K.H. Harib, A Stochastic Model for Simulating Cutting Forces, *Proceedings of the 6th CIRP International Conference on Intelligent Computation in Manufacturing Engineering*, 23-25 July, 2008, Naples, Italy, p.343-348.

A.M.M.S. Ullah and K.H. Harib, Simulation of cutting force using nonstationary Gaussian process, Journal of Intelligent Manufacturing, In Press, DOI:10.1007/s10845-009-0245-2.

J.A. Ibarbia, A. Diez, R. N.-Silva, A. R. Campos, D. Stokic, A. Correia, Ambient Intelligence for supporting the Collaborative Working Environment in Manufacturing, *Proceedings of the 6th CIRP International Conference on Intelligent Computation in Manufacturing Engineering*, 23-25 July, 2008, Naples, Italy, p.591-596.

J. D. Cogdell, A convolved multi-Gaussian probability distribution for surface topography applications, *Precision Engineering*, Vol.32(1), 2008, p.34-46.

K.K. Manesh, B. Ramamoorthy, M. Singaperumal, Equation Numerical generation of anisotropic 3D non-Gaussian engineering surfaces with specified 3D surface roughness parameters, *Wear*, In Press, DOI:10.1016/j.wear.2010.02.005.

A.M.M.S. Ullah, K.H., Harib and S. Aldajah. On the Roughness Profile Modeling using Q-Sequence, *Proceeding of the Ninth CIRP Workshop on Modeling of Machining Operations*, 11-12, May 2006, Bled, Slovenia p.431-437.

A.M.M.S. Ullah and K.H. Harib, Knowledge extraction from time series and its application to surface roughness simulation, *Information Knowledge Systems Management*, 5, 2006, 117-134.